THE IMPACT OF AIR-FLOW SEPARATION ON THE DRAG OF THE SEA SURFACE

V. N. KUDRYAVTSEV
Marine Hydrophysical Institute, Sebastopol, Ukraine

V. K. MAKIN
Royal Netherlands Meteorological Institute (KNMI), De Bilt, The Netherlands

(Received in final form 13 June 2000)

Abstract. An approach that allows assessment of the impact of air-flow separation (AFS) from wave breaking fronts on the sea-surface drag is presented. Wave breaking fronts are modelled by the discontinuities of the sea-surface slope. It is assumed that the dynamics of the AFS from wave breaking crests is similar to that from the backward facing step. The form drag supported by an individual breaker is described by the action of the pressure drop distributed along the forward face of the breaking front. The total stress due to the AFS is obtained as a sum of contributions from breaking fronts of different scales. Outside the breaking fronts the drag of the sea surface is supported by the viscous surface stress and the wave-induced stress. To calculate the stress due to the AFS and the wave-induced stress a physical model of the wind-wave spectrum is used. Together with the model of the air flow described in terms of surface stresses it forms a self-consistent dynamical system for the sea surface-atmosphere where the air flow and wind waves are strongly coupled. Model calculations of the drag coefficient agree with measurements. It is shown that the dimensionless Charnock parameter (roughness length normalized on the square of the friction velocity and the acceleration of gravity) increases with the increase of the wind speed in agreement with field measurements. The stress due to the AFS normalized on the square of the friction velocity is proportional to the cube of wind speed. At low winds the viscous surface stress dominates the drag. The role of the form drag, which is the sum of the stress due to the AFS and the wave-induced stress, is negligible. At moderate and high winds the form drag dominates. At wind speeds higher than 10 m s^{-1} the stress supported by the AFS becomes comparable to the wave-induced stress and supports up to 50% of the total stress.

Keywords: Air-flow separation, Breaking wind waves, Sea drag.

1. Introduction

There is increasing experimental evidence that breaking waves play a significant role in the dynamics of the lower atmosphere and the upper ocean (see, for example, a review by Melville, 1996). For air-flow dynamics, the understanding of how breaking waves impact upon the exchanges of momentum, heat and gas through the sea surface is of primary importance. A significant augmentation of the surface local stress above breaking waves is reported in laboratory experiments (Banner, 1990; Banner and Melville, 1976; Kawamura and Toba, 1988; Giovanangeli et al., 1999; Reul et al., 1999). In these studies it has been established that

Boundary-Layer Meteorology **98:** 155–171, 2001.

air-flow separation (AFS) from the crest of breaking waves is responsible for this augmentation. Wave breaking manifests itself in whitecapping, a ubiquitous and commonly observed phenomenon on the sea surface. At high winds whitecapping is very intensive, and suggests that air-flow separation may play a significant role in the air-flow dynamics above waves and, consequently, in exchange processes at the sea surface.

The main goal of the present paper is to develop an approach that allows the impact of air-flow separation from breaking waves on the sea drag to be taken into account. To that end we assume that the impact of air-flow separation on the momentum flux can be described as the action of a strong drop of pressure distributed along the wave breaking fronts. It is assumed that the dynamics of the air flow separated from the breaking crest of an individual wave is similar to that which occurs over the backward facing step. This picture emerges from the experimental study by Reul et al. (1999; see also Giovanangeli et al., 1999) where the kinematics of the separated air flow has been controlled visually with the use of Particle Image Velocimetry (PIV) system. Figure 1 from Reul et al. (1999) visualizing the breaking wave suggests the analogy with the backward facing step. We distinguish this 'separation' stress from the wave-induced stress. The latter is formed by the non-separated air flow over a regular water-wave profile and can be described in terms of the wave growth-rate parameter (e.g., the sheltering mechanism of the wind-wave interaction by Belcher and Hunt (1993)). The former is associated with the wave breaking when the sea surface is disrupted and the process is highly unsteady and evolves rapidly. The sum of these two stresses determines the form drag at the sea surface, that is, the correlation of the surface pressure with the surface slope. The form drag together with the viscous stress forms the total stress (momentum flux) at the sea surface.

In the coupled sea surface-atmosphere model developed by Makin and Kudryavtsev (1999) and Kudryavtsev et al. (1999) the air-flow separation mechanism was not taken into account in the description of the sea drag. Here we extend the coupled model by accounting for the separation stress in the form drag. We use a somewhat simplified approach based on the integral-over-height conservation equation for the horizontal momentum to describe the wind-wave coupling. The model by Makin and Kudryavtsev (1999) is based on the differential conservation equation. The advantage of the present approach is that we do not need to resolve the vertical structure of the wave boundary layer as was done in the model by Makin and Kudryavtsev (1999). We anticipate that the air flow separation changes drastically the vertical structure of stresses near the wave surface. The details of this impact is not known. Instead of speculating on how to parameterize the vertical structure of the wave boundary layer influenced by air-flow separation we apply here an integral (bulk) approach. The integral approach is not sensitive to the details of the wind profile just above the waves so that we can approximate the wind profile by the logarithmic distribution. We thus neglect the deviation of the wind profile

caused by the waves from the logarithmic distribution, which we have accounted for in Makin and Kudryavtsev (1999).

In our model the air-flow separation stress is related to the statistical properties of the wave breaking fronts described in terms of $\Lambda(\mathbf{c})\,d\mathbf{c}$ – the average total length per unit surface area of breaking fronts that have velocities in the range $\mathbf{c}$ to $\mathbf{c} + d\mathbf{c}$. This wave breaking statistic was introduced originally by Phillips (1985), who related this quantity to the rate of energy dissipation due to wave breaking. To avoid the poorly known quantity $\Lambda(\mathbf{c})$ in the description of air-flow separation we instead use the rate of energy dissipation. The advantage of this approach is that the rate of energy dissipation can be estimated from the energy balance in the equilibrium range of the wind-wave spectrum. We further assume that the rate of energy dissipation is proportional to the energy input from the wind. In this case the air-flow separation stress can be directly related to the saturation wave spectrum and knowledge of the wave breaking statistics is not required.

The second goal of the paper is to assess the role of air-flow separation in the formation of sea drag for a fully developed sea. To provide an estimate of the impact of the AFS on the total stress we use the saturation wave spectrum model developed by Kudryavtsev et al. (1999). It is shown that the role of the AFS in supporting the surface stress increases rapidly with increasing of the wind speed. At 20 m s^{-1} and higher the AFS contributes more than 40% of the total stress. We compare the model drag coefficients with the open ocean data and show an overall agreement. Due to the impact of the AFS the sea-roughness parameter being expressed in terms of the Charnock 'constant' increases by a factor of two in the wind speed range 10 m s^{-1} to 20 m s^{-1}. This is in agreement with recent measurements by Yelland and Taylor (1996).

2. Drag Supported by the Air-Flow Separation from Breaking Crests of Narrow Band Surface Waves

We consider the turbulent air flow above the sea surface

$$z = \zeta(t, x, y),$$

where (x, y, z) is the Cartesian coordinate system, the x-axis coincides with the mean wind direction, and z is directed upward. We assume that the turbulent air flow is stationary and spatially homogeneous. The conservation equation for the x-component of the horizontal momentum integrated over z from the sea surface to a level h and spatially averaged has the form

$$u_*^2 = \tau^\nu + \overline{p\frac{\partial \zeta}{\partial x}}, \tag{1}$$

where τ^ν is the viscous stress at the surface, p is the surface pressure, the friction velocity of the air squared u_*^2 is the turbulent momentum flux at height $z = h$,

chosen far above the surface so that the wave-induced flux is negligible there, and the overbar denotes the spatial averaging. The stresses in (1) are normalized on the air density.

We first consider a case when the sea surface is presented as a superposition of random surface waves with the wavenumber in the range $\mathbf{k}$ to $\mathbf{k} + \mathrm{d}\mathbf{k}$. When this random surface approaches the critical height a_b the wave crest breaks. Wave breaking fronts run with velocities in the range $\mathbf{c}$ to $\mathbf{c} + \mathrm{d}\mathbf{c}$. The speed of the wave breaking front and the wavenumber of the surface wave are related by the linear dispersion relation $c^2 = g/k$ (g is the acceleration due to gravity), and the direction of the breaking front velocity coincides with the wavenumber vector.

We assume that the sea surface can be presented as a streamlined surface covered by areas where the air-flow separation takes place. The air-flow separation occurs intermittently on the sea surface where wave breaking fronts arise. In the vicinity of the breaking crest the local surface slope is very sharp. Let us describe a breaking front on the sea surface at a given moment $t = t_0$ as a curved line on the (x, y) plane

$$y = \xi_i(x, t_0). \tag{2}$$

Then the mapping of the wave breaking fronts on the surface-slope plane can be presented as a discrete number of the slope discontinuity, which is located on lines (2). We shall model each slope discontinuity as the delta-function

$$(\partial\zeta/\partial x)_i = 2a_b\delta(y - \xi_i(x)), \tag{3}$$

where the surface displacement difference over each slope discontinuity is assumed to be the same and equal to the height $2a_b$ of the breaking wave with amplitude a_b.

After substitution of (3) into the second term on the right-hand side of (1), and averaging the obtained equation over the area S, the form drag can be written as

$$\overline{p\frac{\partial\zeta}{\partial x}} = \overline{\tilde{p}\frac{\partial\tilde{\zeta}}{\partial x}} + 2a_b\Delta p_s\cos\theta_b\frac{1}{S}\sum_N l_i. \tag{4}$$

Here Δp_s is the drop of the surface pressure on the forward side of the breaking front, $\sum l_i$ is the total length of wave breaking fronts running with velocities in the range $\mathbf{c}$ to $\mathbf{c} + \mathrm{d}\mathbf{c}$ (the total length of the surface slope discontinuity), θ_b is the angle between the normal to the breaking front and the x-axis, N is the number of breaking fronts in the area S, and the tilde denotes a variable related to the streamlined surface.

The first term on the right-hand side of (4) describes the momentum transfer from wind to waves by the wave-induced pressure. This flux is traditionally expressed in terms of the directional wave variance spectrum $F(\mathbf{k})$ and the growth rate parameter β

$$\overline{\tilde{p}\frac{\partial\tilde{\zeta}}{\partial x}} \equiv \tau^w = \beta\cos\theta\omega^2 F(\mathbf{k})\,\mathrm{d}\mathbf{k}, \tag{5}$$

where θ is the direction of the wavenumber vector $\mathbf{k}$.

The second term on the right-hand side of (4) describes the form drag produced by the AFS. This term has a clear physical sense if the analogy between the aerodynamics of the air flow over the breaking wave and the backward facing step (Reul et al., 1999) is accepted. The horizontal force acting on the vertical forward face of the individual breaker front with area $2a_b l$ is proportional to $2a_b l \Delta p_s$. The term in (4) is then the horizontal force per unit surface averaged over all breaking fronts and having the same height. The quantity $(1/S)\sum l_i$ is the average total length of breaking fronts per unit surface introduced originally by Phillips (1985)

$$\frac{1}{S}\sum l_i = \Lambda(\mathbf{c})\,\mathrm{d}\mathbf{c}, \tag{6}$$

where the distribution $\Lambda(\mathbf{c})$ represents the surface density of the total length of wave breaking fronts that have velocities in the range $\mathbf{c}$ to $\mathbf{c}$ + d$\mathbf{c}$. The drop of pressure induced by the separation acts on the wave breaking front during a short period of time and then disappears. The pressure drop can be estimated by using the analogy between the AFS from breaking waves and separated flows typical of the backward facing step. This analogy was suggested by Reul et al. (1999) who studied experimentally the kinematics of the separated air flow from breaking waves by means of the PIV approach. The visualization of the AFS event from the breaking wave presented in their Figure 1 clearly supports the analogy with the backward facing step. The separated flows from the backward step were studied extensively in the laboratory (see, e.g., review by Simpson, 1989; and Chandrsuda and Bradshaw, 1981). The pressure drop is parameterized as

$$\Delta p_s = \frac{1}{2}\gamma (U_s \cos\theta_b - c)^2, \tag{7}$$

where γ is an empirical constant, U_s is the mean wind speed related to some reference level, and θ_b is the angle between the direction of the moving wave breaking front and the wind. The angle accounts for the fact that only the component of the wind velocity perpendicular to the wave breaking front is responsible for the airflow separation. Because the breaking front moves with speed c the pressure drop is proportional to the relative wind speed $U_s \cos\theta_b - c$ and not to the reference wind speed U_s. To estimate the reference wind speed we use the logarithmic wind profile

$$U(z) = \frac{u_*}{\kappa}\ln\frac{z}{z_0}, \tag{8}$$

where z_0 is the roughness length to be found. The reference level for U_s is specified as a level just above the breaking crest, i.e., at $z = a_b = \varepsilon_b/k$, where $\varepsilon_b = a_b k$ is the slope of the breaking wave. The pressure drop (7) can now be estimated as

$$\Delta p_s = \gamma \frac{u_*^2}{2\kappa^2}\ln^2(\varepsilon_b/kz_c)\cos^2\theta_b, \tag{9}$$

where $z_c = z_0 \exp(\kappa c/(u_* \cos\theta_b))$ is traditionally referred to as the height of the critical layer. Finally, the drag of the sea surface supported by the air-flow separation from the breaking crests of the narrow band surface waves $\tau_s(\zeta)$ is

$$\tau^s = (\varepsilon_b \gamma/\kappa^2) u_*^2 \ln^2(\varepsilon_b/kz_c) \cos^3\theta_b k^{-1} \Lambda(\mathbf{c})\, d\mathbf{c}. \tag{10}$$

To evaluate Equation (10) we have to specify constants ε_b and γ, and to define the distribution function $\Lambda(\mathbf{c})$. The characteristic value of the wave breaking slope can be estimated from laboratory measurements as $\varepsilon_b = 0.3 - 0.6$ (e.g., Banner, 1990; Kawamura and Toba, 1988; Reul et al., 1999). Constant γ defines the drop of pressure on the forward face of the breaking front. As was already discussed, the dynamics of the separation region associated with the breaking wave crest is very similar to that on the backward facing step as suggested by Reul et al. (1999). Chandrsuda and Bradshaw (1981) give an estimate of $\gamma \approx 1$ in their study of the reattaching flow over the backward facing step. We shall accept this estimate for the present study.

We can now estimate the drag due to the AFS in the extreme case of a monochromatic slow wave $c \ll U_s$, so steep that each of its crests breaks. In this case the distribution

$$\Lambda(\mathbf{c})\, d\mathbf{c} = \frac{1}{2\pi} k. \tag{11}$$

If we assume that the drag in this case is completely supported by the air-flow separation it follows from (1) and (10) that $\varepsilon\gamma/(2\pi\kappa^2) \log^2(\varepsilon_b/kz_0) = 1$. This results in the estimate of the roughness parameter

$$\frac{z_0}{h_b} = \frac{1}{2} \exp\left(-\kappa \sqrt{\frac{2\pi}{\varepsilon_b \gamma}}\right), \tag{12}$$

where $h_b = 2a_b$ is the height of the breaking wave. Behind the backward facing step the separation bubble is well pronounced (Chandrsuda and Bradshaw, 1981) and γ is close to 1. Behind the crests of breaking waves following each other the separation zone is less pronounced and γ should be less than 1. We take $\gamma = 0.1 \div 1.0$. With $\varepsilon_b = 0.5$ the roughness scale is $z_0/h_b = 0.01 \div 0.1$. This estimate is consistent with the empirical knowledge (for example, Monin and Yaglom, 1971) that z_0 for very rough surfaces is about 1/30 of the characteristic height of the roughness elements.

3. Drag of the Sea Surface Accounting for the AFS

Let us rewrite the momentum conservation equation (1) in the form

$$u_*^2 = \tau^\nu + \tau^w + \tau^s. \tag{13}$$

In (13) the wave-induced flux (5) and the flux supported by the AFS (10) should be integrated over the wavenumber domain of wind waves

$$\tau^s = (\varepsilon_b \gamma/\kappa^2) u_*^2 \int_{\mathbf{c}} \ln^2(\varepsilon_b/kz_c) \cos^3\theta_b k^{-1} \Lambda(\mathbf{c}) \mathbf{dc}, \tag{14}$$

and

$$\tau^w = \int_k \int_\theta \beta c^2 B(k,\theta) \cos\theta d \ln k \, \mathrm{d}\theta, \tag{15}$$

where $B = k^4 F$ is the saturation wave spectrum. The growth rate parameter β in (15) is specified in the form

$$\beta = C_\beta \left(\frac{u_*}{c}\right)^2 \cos^2\theta, \tag{16}$$

where C_β is the proportionality coefficient. Plant (1982) has analyzed several laboratory and field experiments and approximated C_β by a constant value $C_\beta = 0.04 \pm 0.02$. In general C_β can be a function of the wavenumber as suggested by, e.g., Stewart (1974) or by Makin and Kudryavtsev (1999). With (16) the relation (15) takes the form

$$\tau^w = u_*^2 \int_k \int_\theta C_\beta B \cos^3\theta d\theta d \ln k. \tag{17}$$

To complete the problem we have to specify the form of the viscous surface stress τ^ν, and to define the distribution function $\Lambda(\mathbf{c})$ in τ^s.

3.1. Viscous Surface Stress

The viscous stress plays the dominant role in the thin molecular sublayer where the turbulent motions are suppressed. The thickness δ of this sublayer in the turbulent boundary layer is

$$\delta = d\frac{\nu}{u_*}, \tag{18}$$

where d is a constant close to 10, ν is the molecular viscosity. The wind velocity profile inside the viscous sublayer is linear

$$U(z) = \frac{\tau^\nu}{\nu} z. \tag{19}$$

We assume that just above the viscous sublayer, at $z > \delta$, the wind profile is logarithmic (8). Patching the wind profiles (19) and (8) at $z = \delta$ we obtain the following definition of the viscous surface stress

$$\tau^{\nu} = (\kappa d)^{-1} \ln(\delta/z_0) u_*^2. \tag{20}$$

If the viscous surface stress is the only component of the total stress (i.e., $\tau^{\nu} = u_*^2$), then (20) defines the roughness scale of the smooth surface

$$\frac{z_0 u_*}{\nu} = d \exp(-\kappa d). \tag{21}$$

With $d = 12$ (the value used in this study) the relation (21) $z_0 \nu / u_* \approx 0.1$, which is the traditional estimate for the dimensionless viscous roughness scale.

3.2. Stress supported by the AFS

To calculate the stress due to the AFS (14) we need to define the distribution of wave breaking fronts $\Lambda(\mathbf{c})$. The description of the statistical properties of the random moving surface is a very complicated problem. The detailed study of the statistical properties of the Gaussian (linear) sea surface was done by Longuet-Higgins (1957). However, the results of that study cannot be applied to our problem as the wave breaking phenomenon is essentially a non-linear process.

We shall follow the approach by Phillips (1985) who has shown that the distribution function $\Lambda(\mathbf{c})$ can be directly related to the average rate of the energy loss D per unit area by breakers with speeds between $\mathbf{c}$ and $\mathbf{c} + d\mathbf{c}$

$$D(\mathbf{c})\, d\mathbf{c} = b g^{-1} c^5 \Lambda(\mathbf{c})\, d\mathbf{c},$$

where b is an empirical constant estimated by Duncan (1981) as $b = 0.03 - 0.07$. Rapp and Melville (1990) give a somewhat lower estimate of $b = 0.003 - 0.016$ for the unsteady breaker. In the present paper we adopt $b \sim 10^{-2}$, accounting for the fact that breaking waves in the sea are essentially unsteady. The approach by Phillips (1985) provides a sufficient advantage for the present study: instead of poorly known function $\Lambda(\mathbf{c})$ the rate of energy dissipation $D(\mathbf{c})$ can be used. Unlike $\Lambda(\mathbf{c})$ the energy dissipation can be easily estimated from the energy balance in the equilibrium range of the wind-wave spectrum.

It is reasonable to assume that under steady conditions the energy dissipation due to wave breaking is equal or proportional to the energy input from the wind in the equilibrium range of the wind wave spectrum, i.e.,

$$D(\mathbf{c}) \sim \beta \omega E(\mathbf{c}), \tag{22}$$

where $E(\mathbf{c})$ is the energy spectrum related to the saturation spectrum as $E(\mathbf{c}) = (\omega^2/k) k^{-4} B(\mathbf{c})$. The total length of wave breaking fronts can be expressed now in terms of the saturation spectrum as

$$\Lambda(\mathbf{c}) \sim \frac{\beta}{b} B(\mathbf{c}) k^{-1}. \tag{23}$$

The shape of the saturation spectrum can be estimated from measurements or calculated from a theoretical model of the wave spectrum. With (23) the separation stress (14) can be written as

$$\tau^s = C_s u_*^2 \int_\theta \int_{k<k_m} \ln^2(\varepsilon_b/kz_c)\beta B \cos^3\theta d\theta d\ln k, \tag{24}$$

where $C_s = \varepsilon_b\gamma/(b\kappa^2)$ is a constant. The integration over the wavenumber k in (24) is done in the wavenumber range satisfying the condition $k < k_m$, where $k_m \sim 2\pi/\lambda_m$ rad m^{-1} and $\lambda_m \sim 0.1$ m. This condition reflects the fact that waves shorter than λ_m tend to generate parasitic capillaries, as discussed by Kudryavtsev et al. (1999). The generation of parasitic capillaries prevents the formation of the sharp surface slope and hence prevents the separation of the air flow over these shorter waves.

Equation (24) directly relates the stress due to the air-flow separation to the statistical properties of wind waves described in terms of the saturation spectrum B. Note, that the uncertainty of C_s in (24) is defined mainly by the uncertainty of constant b. Fortunately, because all constants are combined in one constant C_s, any change in one constant can be compensated by the change in the others.

To give a preliminary estimate of the separation stress according to (24) we have to specify the shape of the saturation spectrum $B(\mathbf{k})$. In a general form the saturation spectrum can be parameterized as

$$B(k,\theta) = \alpha_0 A(\theta)\left(\frac{u_*}{c}\right)^m, \tag{25}$$

where α_0 is a saturation constant, $A(\theta)$ is an angular distribution function (equal to 1 at $\theta = 0$), and m is the wind exponent. According to field measurements the wind exponent for the short gravity waves can vary from $m = 0.18 \pm 0.18$ (Banner et al., 1989) to $m = 1$ (Toba, 1973). The wind exponent found from laboratory measurements by Jähne and Riemer (1990) equals 1 for short gravity waves. Let us substitute the spectrum (25) into (24). Taking into account that the integral converges at the upper limit of k, and that the angular distribution of the spectrum is significantly broader than $\cos^5\theta$, the following estimate for the separation stress is obtained

$$\frac{\tau^s}{u_*^2} \approx \left(\frac{\alpha_0 C_s}{2+m}\right)\ln^2(\varepsilon_b/k_m z_0)\left(\frac{u_*}{c_m}\right)^{2+m}, \tag{26}$$

where c_m is the phase velocity at $k = k_m$. Taken $\varepsilon_b = 0.5$, $\gamma = 1.0$, and $b = 0.01$, constant C_s is $C_s \approx 300$. Defining the growth rate constant $C_\beta = 0.04$, and the saturation constant α_0 to be in the range $\alpha_0 = 10^{-3} \div 10^{-2}$, and specifying for the definition $\log(k_m z_0) = -2$, we finally get

$$\tau^s/u_*^2 \sim (0.1 \div 1)\cdot(u_*/c_m)^{2+m}. \tag{27}$$

This relation shows that the impact of air-flow separation on the sea drag is negligible at low winds and rapidly increases with increasing wind speed. At high winds one can expect that the AFS plays the dominant role in the formation of the sea drag. The value of τ^s according to (27) is not sensitive to the lower limit of the integration in (24). From the physical point of view this fact means that breaking of short gravity waves dominates the stress supported by the AFS. Although the drag of the individual small-scale breaker is small their contribution to the separation stress dominates the contribution from the large-scale breakers due to their high surface density.

4. Results

In the previous section we have considered all the components of the stress that support the surface drag: the wave-induced stress τ^w, the viscous stress τ^ν, and the separation stress τ^s (Equations (17), (20), and (24) correspondingly). It is important to notice that the model predicts two asymptotic aerodynamic regimes of the air flow: the smooth one (21), and the rough one (12).

The resistance law of the sea surface results from (13) with (17), (20), and (24)

$$\int_k \int_\theta C_\beta B \cos^3\theta d\theta d\ln k + C_s \int_\theta \int_{k<k_m} C_\beta \ln^2\left(\frac{\varepsilon_b}{kz_c}\right)\left(\frac{u_*}{c}\right)^2 B\cos^5\theta d\theta d\ln k + (\kappa d)^{-1}\ln(\delta/z_0) = 1. \tag{28}$$

The resistance law relates the roughness parameter of the sea surface z_0 (or the drag coefficient) to the statistical properties of the sea surface in terms of the saturation spectrum.

4.1. Specification of $B(k,\theta)$ and C_β

To obtain the roughness parameter as a function of wind speed according to (28) an empirical wave spectrum or a physical model of the wave spectrum can be used. To calculate the stress due to the AFS, the equilibrium part of the wave spectrum defined at $k < k_m$ has to be known, and the calculation of the wave-induced stress τ^w requires the shape of the spectrum in the wavenumber range from capillary waves to the spectral peak. Here we use a physical model of the wave spectrum developed by Kudryavtsev et al. (1999), which describes the saturation spectrum $B(k,\theta)$ in the full wavenumber range from a few millimetres up to the spectral peak. It consists of two parts: the low and the high wavenumber spectrum

$$B(k,\theta) = B_l(k,\theta) + B_h(k,\theta). \tag{29}$$

The shape of the low wavenumber spectrum B_l is defined by the empirical model of Donelan et al. (1985) with the correction proposed by Elfouhaily et al. (1997). The shape of the high wavenumber spectrum B_h results from the energy balance of wind input, viscous dissipation, dissipation due to wave breaking (including energy losses due to generation of parasitic capillaries by short gravity waves), and non-linear three-wave interaction. In the equilibrium range of short gravity waves we follow Phillips (1985) and assume that dissipation due to wave breaking (and consequently the distribution function of wave breaking fronts) can be parameterized as a cube of the saturation spectrum. The shape of the saturation spectrum B_h in this range results from the balance between wind input and dissipation due to wavebreaking. In the capillary range, the shape of the spectrum B_h is defined by the balance between viscous dissipation and cascade energy transfer from short gravity waves (the mechanism of generation of parasitic capillaries). The details of the model of the wave spectrum (29) can be found in Kudryavtsev et al. (1999).

Now we need to specify the function C_β, which appears in the resistance law (28). In the present paper it is parameterized in the form proposed by Stewart (1974), and as used by Makin et al. (1995)

$$C_\beta = a_1 \rho_w / \rho_a \kappa^{-1} \ln(\pi / k z_c), \tag{30}$$

where ρ_w, ρ_a are the density of water and air, and the value of a_1 is of the order 1. The parameterization of β in the form (16) with (30) differs from that proposed by Makin and Kudryavtsev (1999). The latter was designed for the vertically resolved wave boundary layer and requires knowledge of the vertical structure of the wave-induced stress. The parameterization of β in the form (16) with (30) was discussed in detail by Makin et al. (1995) where it was shown that with $a_1 = 2$ (the value used here) it closely follows the empirical relation of Plant (1982) with $C_\beta = 0.04 \pm 0.02$.

4.2. Model calculations

For a given wind speed the solution of Equation (28) provides the sea surface roughness parameter z_0, which is a function of the saturation spectrum B. The saturation spectrum B_h in turn depends on the momentum flux, which is defined by the sea-surface roughness z_0. Thus the wind waves and the atmospheric boundary layer are strongly coupled forming a self-consistent dynamical system. The model results are obtained with the reference speed $U(h)$ traditionally taken at $h = 10$ m. Equation (28) with the given model of the saturation spectrum $B(k, \theta)$ is solved by iterations.

We first illustrate how the stress due to the AFS affects the coupled wind-wave – turbulent air-flow system. To do that we compare the model calculations with and without accounting for the stress due to AFS. The latter calculations are comparable to those presented in Kudryavtsev et al. (1999), where the deviation of the

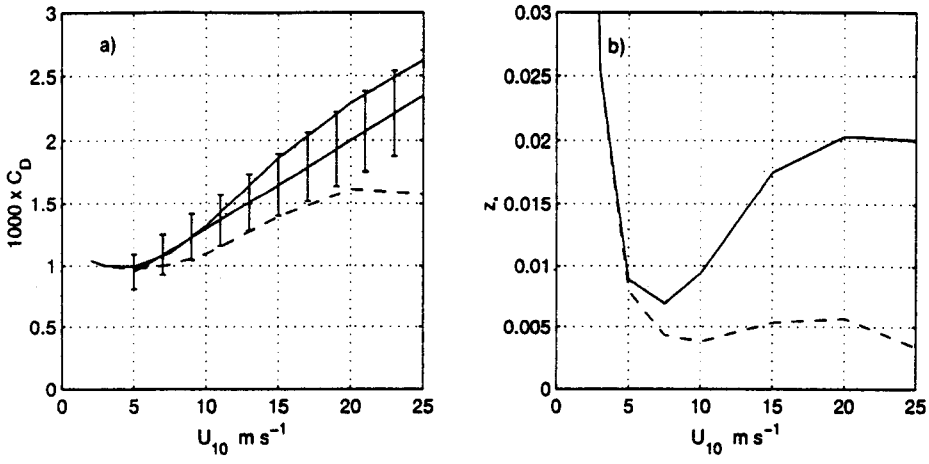

Figure 1. Model results: solid line, separation stress is accounted for; dashed line, separation stress is not accounted for. (a) Drag coefficient versus U_{10}. Dashed-dotted line, regression from Yelland and Taylor (1996) with 15% error bars; (b) Charnock parameter $z_0 g/u_*^2$ versus U_{10}.

wind profile from the logarithmic one due to the vertical distribution of the wave-induced momentum flux was taken into account. The present model is based on the momentum conservation Equation (13) integrated over height. The difference between two models is independent of the physical approach taken to describe the problem.

The model calculations presented below are obtained with the model constants $\varepsilon_b = 0.5$, $\gamma = 1.0$ and $b = 0.01$. The maximal wavenumber of breaking waves over which the AFS occurs is $k_m = 2\pi/0.05$ rad m^{-1}. The tuning constants of the short wind-wave number spectrum B_h are chosen so that the mean square slope resulting from the model fits the values observed by Cox and Munk (1954) (see Kudryavtsev et al. (1999) for details). The correspondence between the modelled and the observed sea-surface slope is essentially important for the present study. The over- or under-estimation of the sea-surface slope (and, consequently, the over- or under-estimation of the wave breaking characteristics) will result in the incorrect estimates of the AFS impact on the sea-surface drag. Notice, that when the stress due to the AFS is not accounted for in the model all the model constants are kept the same.

In Figure 1 the drag coefficient $C_D = (u_*/U_{10})^2$ and the dimensionless roughness length $z_* = z_0 g/u_*^2$ (the so-called Charnock parameter) for the developed seas specified by the inverse wave age parameter $U_{10}/c_p = 0.83$ (c_p is the phase speed at the spectral peak) are shown as a function of the wind speed. The solid lines represent the solution of the full model (the stress due to the AFS is accounted for), while the dashed ones represent the model solution when the stress due to the AFS is not accounted for. We first compare the model results with the recent open ocean data (fully developed seas) of Yelland and Taylor (1996). Considering the

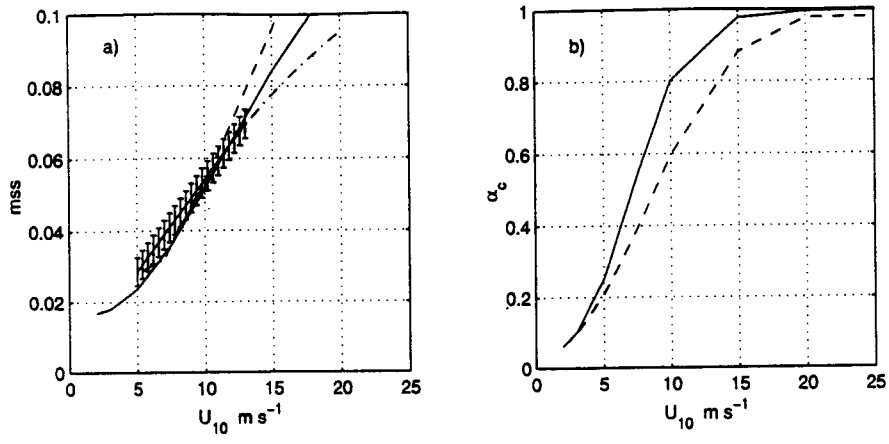

Figure 2. (a) The same as in Figure 1, but for the mean square slope (mss). Regression of Cox and Munk (1954) is shown by dashed-dotted line with errorbars; (b) The same as in Figure 1, but for the coupling parameter α_c.

standard error of 15–20% in the stress measurements (Donelan, 1990), and thus in C_D, the overall agreement between the model results and data is reasonable. When the separation stress is switched off the model underpredicts the drag coefficient for high winds. As anticipated the AFS enhances the drag of the sea surface. The AFS impact increases with the increase of the wind speed. At high winds the drag coefficient C_D resulting from the full model exceeds the drag coefficient resulting from the wave-induced stress alone up to about 50%. The additional stress supported by the AFS is responsible for the well pronounced wind speed dependence of the Charnock parameter z_* shown in Figure 1b. In the range of the wind speed from 10 to 20 m s^{-1} the Charnock parameter increases by a factor of 2 in correspondence with field measurements (for example, see Figure 10a in Yelland and Taylor (1996), where z_* increases from 0.011 to 0.017). A strong increase of the Charnock parameter at low winds reflects the transition of the sea surface from the aerodynamically rough to the smooth condition. At low winds the surface viscous stress (20) dominates the surface drag and the roughness length is described by (21).

The short wind-wave spectrum results as a solution of the coupled model. The most important integral characteristic of the short wind waves, the mean square slope, is shown in Figure 2a as a function of the wind speed. The mean square slope resulting from the full model compares reasonably with the Cox and Munk (1954) data. When the stress due to the AFS is switched off the mean square slope exceeds the full model prediction at high winds. The reason for this becomes clear if we consider the growth rate parameterization (16) with (30). The decrease of the surface drag when the stress due to AFS is switched off results in the decrease of u_* and in the increase of C_β due to the decrease in the roughness length. At high wind speeds, $U > 15$ m s^{-1}, the role of the latter effect is stronger in the

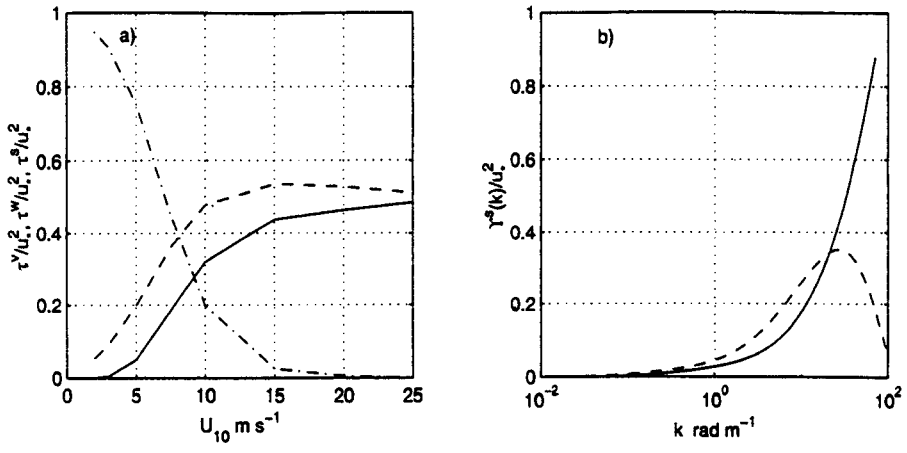

Figure 3. (a) Stress contributions. Solid line, stress due to separation τ^s/u_*^2; dashed line, wave-induced stress τ^w/u_*^2; dashed-dotted line, viscous stress τ^v/u_*^2; (b) Spectrum of separation stress versus wavenumber k. Solid line, wind speed $U_{10} = 10$ m s^{-1}; dashed line, $U_{10} = 25$ m s^{-1}.

wavenumber range forming the mean squared sea slope. At lower winds these two factors compensate each other and there is no noticeable difference between the two model calculations.

The coupling parameter α_c, defined as the ratio of the form drag to the total drag u_*^2, is shown in Figure 2b. For the full model the coupling parameter is $\alpha_c = (\tau^s + \tau^w)/u_*^2$, while $\alpha_c = \tau^w/u_*^2$ when the stress τ^s is switched off. The wind-speed dependence of the coupling parameter in both cases is roughly the same. At high wind speeds most of the drag is due to the form drag, while at low wind speeds the viscous stress dominates.

To illustrate the role of air-flow separation in the momentum transfer the contribution to the total stress u_*^2 of the viscous stress τ^v/u_*^2, the wave-induced stress τ^w/u_*^2, and the stress due to the AFS τ^s/u_*^2 as a function of the wind speed is shown in Figure 3a. Notice, that $\tau^v/u_*^2 + \tau^w/u_*^2 + \tau^s/u_*^2 = 1$. For low wind speeds, $U < 5$ m s^{-1}, the viscous stress dominates the sea-surface drag while the role of the form drag is negligible. With the increase of the wind speed the role of the form drag becomes pronounced. At wind speeds > 10 m s^{-1} the surface drag is mainly supported by the wave-induced and the AFS stresses. The relative role of the stress due to the AFS increases with increase in wind speed and for high wind speeds it supports about 50% of the total stress.

Figure 3b shows the spectral contribution of wave components to the stress due to the AFS (spectrum of τ^s) defined as

$$\Upsilon^s(k)/u_*^2 = C_s \int_\theta \ln^2(\varepsilon_b/kz_c)\beta(k,\theta)B(k,\theta)\cos^3\theta \mathrm{d}\theta$$

so that $\tau^s = \int \Upsilon^s(k) d\ln(k)$. As was mentioned above, at moderate wind speed, $U \approx 10$ m s^{-1}, the main contribution to the separation stress comes from the

shortest gravity waves due to the high surface density of their breaking crests. However, at high wind speeds ≈ 25 m s^{-1} the maximum of the separation stress is shifted toward longer waves. This fact is due to enhanced surface roughness, which decreases the relative speed of the air flow separated from the crest of shortest gravity waves and thus the separation stress associated with these waves. This shows that at high wind speeds where the AFS stress dominates the surface drag the model results are insensitive to the upper limit of the integration in (24).

5. Summary

In the present paper we have proposed an approach that allows explicit assessment of the impact of air-flow separation from wave breaking crests on the sea-surface drag. The approach is based on the momentum conservation equation integrated over height from the sea surface to a level far enough above the surface so that the correlation of the air flow with the wave surface is lost. The sea surface is viewed as a streamlined surface covered by a discrete number of wave breaking fronts, which are modelled by the surface slope discontinuity. Outside breaking fronts the momentum transfer from the air flow to the sea surface is realized through the viscous stress and the momentum flux to waves described in terms of the growth rate parameter.

It is assumed that the dynamics of the separated air flow over breaking waves is similar to that over the backward facing step. The experimental evidence of such similarity has been found in laboratory experiments by Reul et al. (1999). In this case the pressure drop on the forward face of the breaking front is proportional to the square of the relative wind velocity at some reference level, and the proportionality coefficient can be estimated from experimental studies of air-flow separation over a backward facing step (e.g., Chandrsuda and Bradshaw, 1981). The stress due to the separation is found as the result of the pressure force on the forward slope of breaking fronts.

Breaking waves represent a random process on the sea surface. In the model the stress due to the air-flow separation is related to the total length of breaking fronts $\Lambda(\mathbf{c})$ per unit surface running with velocities in the range from $\mathbf{c}$ to $\mathbf{c} + \mathrm{d}\mathbf{c}$. This parameter of the wave breaking statistics was originally introduced by Phillips (1985). He also showed that the energy dissipation due to wave breaking can be expressed via the distribution function $\Lambda(\mathbf{c})$. To avoid the use of the poorly known function $\Lambda(\mathbf{c})$ in the model we followed Phillips (1985) and replaced the distribution function $\Lambda(\mathbf{c})$ by the energy dissipation function $D(\mathbf{c})$. The use of the energy dissipation D instead of Λ in the model has an advantage, since it can be estimated from the energy balance of wind waves. Assuming that D is proportional to the wind input, we directly related the stress supported by the AFS to the saturation wave spectrum.

The viscous stress, the wave-induced stress, and the stress supported by the air-flow separation are three components that form the sea-surface drag. The sum of the last two stresses is the form drag, that is, the correlation of the surface pressure with the surface slope, and is directly related to waves described statistically in terms of the directional wavenumber spectrum. The physical model of the wind-wave spectrum proposed by Kudryavtsev et al. (1999), together with the description of the atmospheric boundary layer in term of stresses, provide a consistent closed dynamical system where the air flow and wind waves are strongly coupled. The vertical momentum flux in the atmospheric boundary layer is to a large extent supported by waves and at the same time determines the growth of waves.

Model calculations of the drag coefficient agree with field measurements. The model shows that the Charnock parameter increases with the increase in the wind speed, in agreement with measurements (e.g., Yelland and Taylor, 1996). This is the impact of the air-flow separation that provides the growth of the Charnock parameter with increasing wind speed. It is shown that at low wind speeds the role of the separation stress (as well as of the wave-induced stress) is negligible, and the surface drag is supported by the viscous surface stress. The contribution of the AFS stress to the total stress u_*^2 increases very fast (as the third power of the friction velocity) with the increase in the wind speed while the contribution of the wave-induced stress is proportional to the first power of the friction velocity. At moderate and high winds the form drag (the sum of the separation and wave-induced stresses) dominates the surface drag. At wind speeds $> 10\ \mathrm{m\ s^{-1}}$ the stress supported by air-flow separation becomes comparable with the wave-induced stress and reaches 50% of the total stress.

We conclude that air-flow separation plays an important role in the formation of the sea-surface drag especially at moderate to high winds. We feel that air-flow separation is one of the central issues in air-sea interaction, the detailed study of which will help to explain many aspects of this complex process.

6. Acknowledgements

We acknowledge the support by the Office of Naval Research under grants ONR N00014-98-1-0437 and N00014-98-1-0653, PR numbers 98PR04572-00 and 98PR05889-00, and by EU INTAS-International Association under grants INTAS-96-1817, INTAS-CNES-97-0222, and INTAS-CNES-97-1291.

References

Banner, M. L.: 1990, 'The Influence of Wave Breaking on the Surface Pressure Distribution in Wind Wave Interaction', *J. Fluid Mech.* **211**, 463–495.

Banner, M. L. and Melville, W. K.: 1976, 'On the Separation of Air Flow above Water Waves', *J. Fluid Mech.* **77**, 825–842.

Banner, M. L., Jones, I. S. F., and Trinder, J. C.: 1989, 'Wavenumber Spectra of Short Gravity Waves', *J. Fluid Mech.* **198**, 321–344.

Belcher, S. E. and Hunt, J. C. R.: 1993, 'Turbulent Shear Flow over Slowly Moving Waves', *J. Fluid Mech.* **251**, 109–148.

Chandrsuda, C. and Bradshaw, P.: 1981, 'Turbulent Structure of a Reattaching Mixing Layer', *J. Fluid Mech.* **110**, 171–194.

Cox, C. S. and Munk, W. H.: 1954, 'Statistics of the Sea Surface Derived from Sun Glitter', *J. Mar. Res.* **13**, 198–227.

Donelan, M. A.: 1990, 'Air–Sea Interaction', *The Sea: Ocean Engineering Science* **9**, 239–292.

Donelan, M. A., Hamilton, J., and Hui, W. H.: 1985, 'Directional Spectra of Wind Generated Waves', *Phil. Trans. Roy. Soc. London, Ser. A* **315**, 509–562.

Duncan, J. H.: 1981, 'An Experimental Investigation of Breaking Waves Produced by Towed Hydrofoil', *Proc. Roy. Soc. London, Ser. A* **377**, 331–348.

Elfouhaily, T., Chapron, B., Katsaros, K., and Vandemark, D.: 1997, 'A Unified Directional Spectrum for Long and Short Wind Driven Waves', *J. Geophys. Res.* **102**, 15,781–15,796.

Giovanangeli, J. P., Reul, N., Garat, M. H., and Branger, H.: 1999, 'Some Aspects of Wind-Wave Coupling at High Winds: An Experimental Study', in *Wind-Over-Wave Couplings*, pp. 81–90, Clarendon Press, Oxford, 356 pp.

Jähne, B. and Riemer, K. S.: 1990, 'Two-Dimensional Wave Number Spectra of Small-Scale Water Surface Waves', *J. Geophys. Res.* **95**, 11,531–11,546.

Kawamura, H. and Toba, Y.: 1988, 'Ordered Motions in the Turbulent Boundary Layer over Wind Waves', *J. Fluid Mech.* **197**, 105–138.

Kudryavtsev, V. N., Makin, V. K., and Chapron, B.: 1999, 'Coupled Sea Surface-Atmosphere Model 2. Spectrum of Short Wind Waves', *J. Geophys. Res.* **104**, 7625-7639.

Longuet-Higgins, M. S.: 1957, 'The Statistical Analysis of a Random Moving Surface', *Phil. Trans. Roy. Soc. London, Ser. A* **249**, 321-387.

Makin, V. K. and Kudryavtsev, V. N.: 1999, 'Coupled Sea Surface-Atmosphere Model 1. Wind over Waves Coupling', *J. Geophys. Res.* **104**, 7613–7623.

Makin V. K., Kudryavtsev, V. N., and Mastenbroek, C: 1995, 'Drag of the Sea Surface', *Boundary-Layer Meteorol.* **79**, 159–182.

Melville, W. K.: 1996, 'The Role of Surface-Wave Breaking in Air–Sea Interaction', *Ann. Rev. Fluid Mech.* **28**, 279–321.

Monin, A. S. and Yaglom, A. M.: 1971, *Statistical Fluid Mechanics*, Vol. 1, MIT Press, Cambridge, 769 pp.

Phillips, O. M.: 1985, 'Spectral and Statistical Properties of the Equilibrium Range in Wind Generated Gravity Waves', *J. Fluid Mech.* **156**, 505–531.

Plant, W. J.: 1982, 'A Relationship between Wind Stress and Wave Slope', *J. Geophys. Res.* **87**, 1961–1967.

Rapp, R. J. and Melville, W. K.: 1990, 'Laboratory Measurements of Deep-Water Breaking Waves', *Phil. Trans. Roy. Soc. London, Ser. A* **331**, 735–800.

Reulm, N., Branger, H., and Giovanangeli, J. P.: 1999, 'Air Flow Separation over Unsteady Breaking Waves', *Phys. Fluids* **11**, 1959–1961.

Simpson, R. L.: 1989, 'Turbulent Boundary-Layer Separation', *Ann. Rev. Fluid Mech.* **21**, 205–234.

Stewart, R.W.: 1974, 'The Air–Sea Momentum Exchange', *Boundary-Layer Meteorol.* **6**, 151–167.

Toba, Y.: 1973, 'Local Balance in the Air–Sea Boundary Processes, III, On the Spectrum of Wind Waves', *J. Ocean Soc. Jpn.* **29**, 209–220.

Yelland, M. and Taylor, P. K.: 1996, 'Wind Stress Measurements from the Open Ocean', *J. Phys. Oceanog.* **26**, 541–558.